Short Circuit Synchronous Electric Charge Extraction (SC-SECE) Strategy for Wideband Vibration Energy Harvesting

Adrien Morel, P. Gasnier, Y. Wanderoild, Gaël Pillonnet, A. Badel

HAL Id: hal-02013371

https://hal.science/hal-02013371

Submitted on 10 Feb 2019

Short Circuit Synchronous Electric Charge Extraction (SC-SECE) Strategy for Wideband Vibration Energy Harvesting

A Morel, P Gasnier, Y Wanderoild, G Pillonnet

Univ. Grenoble Alpes, F-38000 Grenoble, France
CEA, LETI, MINATEC, F-38054 Grenoble, France
adrien.morel@cea.fr

A Badel

Univ. Savoie Mont Blanc, SYMME,
F-74000 Annecy, France

Abstract— **This paper presents an energy harvesting strategy called Short Circuit Synchronous Electric Charge Extraction (SC-SECE), which is an improvement of the SECE strategy for highly coupled piezoelectric generators. The SC-SECE strategy is based on the control of a short-circuit through two tuning parameters. The first one, ϕ_S, represents the phase between the displacement extrema and the energy harvesting event. The second, $\Delta\phi$, is the angle difference between the beginning and end of the short-circuit phase. The performance of this strategy has been compared to other interfaces such as the SECE and the capacitance tuning approach. However, with the SC-SECE strategy, both the power and bandwidth are greatly improved. Experimental measurements have been performed on a highly-coupled piezoelectric harvester (k_m^2=0.48) which provides a maximal harvestable power P_{lim} of 6µW under an extremely low vibration amplitude (0.03G). We have been able to harvest more than 50% of this P_{lim} over a large frequency band, from 90Hz to 140Hz. These results demonstrate the excellent potential of this strategy for extending the bandwidth of piezoelectric vibration energy harvesters.**

Keywords - Vibration Energy Harvesting, Multiphysics modelling, Piezoelectricity, Interface circuit, Short-circuit control, SECE.

I. INTRODUCTION

Over the last two decades, scavenging ambient energy has been investigated as a possible replacement of or complement to batteries in order to make small systems and sensors autonomous [1]. Piezoelectric energy harvesting is particularly interesting in closed and confined environments where temperature gradients and solar light are insufficient to supply a sensor. One of the main building blocks of a piezoelectric energy harvester (PEH) is the interface circuit which has to optimize the extraction of the energy stored in the piezoelectric material. Several synchronous strategies have been proposed, exhibiting high performances for lowly-coupled piezoelectric harvesters [2-5]. However, for highly-coupled PEH's , those strategies are no longer optimal since they overdamp the mechanical resonator [2,6]. In order to match the damping induced by the electrical interface with the mechanical one and enhance the energy extraction process for highly-coupled systems, new strategies have recently been proposed [6,7]. Some of these even induce a tuning of the resonant

frequency over a certain frequency range [8,9]. However, we propose a new strategy called SC-SECE based on a short-circuit tunable phase which allows optimization of the harvested energy while improving the frequency tuning range compared to other state-of-the-art interfaces. Instead of accumulating the energy in the piezoelectric material during a whole semi-period as in the SECE approach, the harvester is short-circuited during a portion of the vibration semi-period. This then decreases the damping induced by the electrical circuit, and also leads to a change in the electromechanical system resonant frequency. In this paper, we first propose an analysis of the effects of a short circuit. Then, we analytically prove that our technique, when associated with highly coupled piezoelectric generators, greatly improves both the harvested energy and the bandwidth compared to the classical SECE strategy. Finally, we validate the theoretical analysis through experimental measurements on a highly-coupled PEH connected to an interface circuit implementing the proposed strategy.

II. MODELING OF THE SC-SECE STRATEGY

A. PEH modeling

A linear PEH is usually composed of a piezoelectric material deposited on a cantilever beam. Applying Newton's law to this mechanical system, we can find the dynamic equation of the mass displacement, x. From the fundamental equations for piezoelectric devices, we can then find the differential equation linking the derivative of the displacement, $\dot{x}$, the piezoelectric voltage, v_p, and the current extracted in the interface circuit, i. Finally, the displacement is considered periodic with a constant amplitude X_m. These three equations are summarized by the system (1).

$$\begin{cases} M\ddot{x} + D\dot{x} + K_{sc}x + \alpha v_p = -\text{F} = -M\ddot{y} \\ i = \alpha\dot{x} - C_p\dot{v}_p \\ x(t) = X_m\cos(\theta) = X_m\cos(\omega t) \end{cases} \quad (1)$$

where y and F are the ambient displacement and vibration force applied on the whole system, respectively. M is the dynamic mass of the system, K_{sc} the short-circuited stiffness, D the mechanical damping of the structure, C_p the piezoelectric clamped capacitance and, finally, α is the electromechanical

coupling between the mechanical part and electrical part of the piezoelectric generator. These equations can be modeled as an equivalent electrical circuit as shown in Fig.1.

B. Expression of the piezoelectric voltage

In order to express the harvested power at every extraction event, we need to solve (1) and find the displacement amplitude, X_m. To do so, we first have to find the expression of the piezoelectric voltage v_p. The piezoelectric element is either working in an open-circuit or short-circuit condition (Fig.2), and hence its voltage expression over a time period can be given by (2).

$$v_p(\theta) = \begin{cases} \dfrac{\alpha}{C_p} \displaystyle\int_{\phi_s+\Delta\phi-\pi}^{\theta} \dot{x}(\theta)d\theta \,, \forall \theta \in\,]\phi_s + \Delta\phi - \pi, \phi_s] \\ \qquad 0 \,, \forall \theta \in\,]\phi_s, \phi_s + \Delta\phi] \\ \dfrac{\alpha}{C_p} \displaystyle\int_{\phi_s+\Delta\phi}^{\theta} \dot{x}(\theta)d\theta \,, \forall \theta \in\,]\phi_s + \Delta\phi, \phi_s + \pi] \\ \qquad 0 \,, \forall \theta \in\,]\phi_s + \pi, \phi_s + \Delta\phi + \pi] \end{cases} \quad (2)$$

$\phi_s \in [0, \pi]$ is the phase between the energy harvesting event and the previous displacement extremum, whereas $\Delta\phi \in [0, \pi]$ represents the angular time spent in the short circuit condition during a semi-period of vibration. A system implementing this extraction strategy is depicted in Fig.1, and an example of the voltage waveform is shown in Fig.2. As given by (2), v_p is non-sinusoidal. In order to analytically solve (1) while simplifying the calculations, only the first harmonic of v_p is considered. Using Fourier series, its expression can be obtained and is given by (3).

$$\begin{cases} v_p(\theta)\big|_{n=1} = a_1 \cos(\theta) + b_1 \sin(\theta) \\ a_1 = \dfrac{2}{\pi} \displaystyle\int_{\phi_s+\Delta\phi-\pi}^{\phi_s+\Delta\phi} v_p(\theta) \cos(\theta)\, d\theta \\ b_1 = \dfrac{2}{\pi} \displaystyle\int_{\phi_s+\Delta\phi-\pi}^{\phi_s+\Delta\phi} v_p(\theta) \sin(\theta)\, d\theta \end{cases} \quad (3)$$
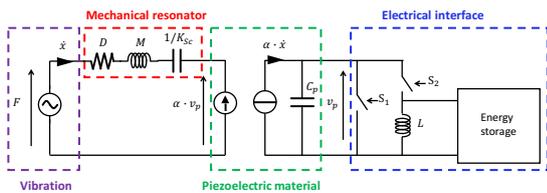

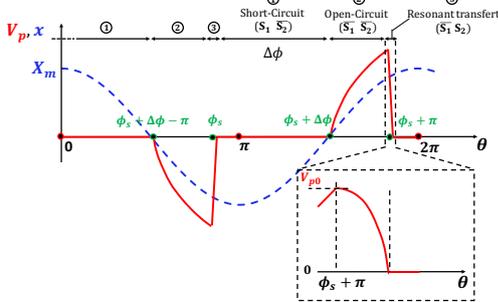Fig. 1. PEH electrical model and system view of the SC-SECE strategy

Fig. 2. Voltage and displacement waveforms of the SC-SECE strategy.

From equations (1), (2) and (3), we obtain the expression of the first Fourier series coefficients, given by (4).

$$\begin{cases} a_1 = \dfrac{\alpha X_m}{\pi C_p}\Big[\pi - \Delta\phi + \dfrac{\sin(2\phi_s + 2\Delta\phi)}{2} + \dfrac{\sin(2\phi_s)}{2} \\ \qquad\qquad + 2\cos(\phi_s + \Delta\phi)\sin(\phi_s)\Big] \\ b_1 = -\dfrac{\alpha X_m}{\pi C_p}[\cos\phi_s + \cos(\phi_s + \Delta\phi)]^2 \end{cases} \quad (4)$$

Thus, the first harmonic of the piezoelectric voltage can be expressed in the Fourier domain as:

$$\underline{v_{p_1}} = \underline{x}\left(\dfrac{a_1}{X_m} - j\dfrac{b_1}{X_m}\right) = \underline{x}(a_1^* - jb_1^*) \quad (5)$$

Where $\underline{x}$ is the displacement written in the Fourier domain, and a_1^* and b_1^* are the first Fourier coefficients a_1 and b_1 divided by the displacement amplitude, X_m.

C. Expression of the harvested power

Considering that only the first voltage harmonic has an impact on the mechanical system dynamic due to the filtering effect of the resonator, we can substitute the voltage expression (5) in (1) in order to find the displacement amplitude. Solving the differential equation in the Fourier domain, we eventually obtain the displacement amplitude, given by (6).

$$\begin{cases} X_m = \dfrac{F}{\sqrt{A^2 + B^2}} \\ A = K_{sc} - M\omega^2 + \alpha a_1^* \\ B = \omega D + \alpha b_1^* \end{cases} \quad (6)$$

For every semi-period, the harvested energy is that stored in the piezoelectric capacitance C_p when $\theta = \phi_s$. Thus, from (1) and (2), the general harvested power expression can be given as a function of the displacement amplitude, as shown in (7).

$$P = \dfrac{\omega\alpha^2}{2\pi C_p} X_m^2 [\cos(\phi_s + \Delta\phi) + \cos(\phi_s)]^2 \quad (7)$$

From (4), (6) and (7), we can now determine the harvested power for any parameter couple $(\phi_s, \Delta\phi)$.

III. MODEL ANALYSIS AND PERFORMANCE ESTIMATION

The energy harvested with a particular extraction strategy is dependent on the PEH used, and varies with the product $k_m^2 Q_m$, where k_m^2 is the modified squared coupling coefficient, and Q_m the mechanical resonator quality factor [2, 10]. It also varies with the normalized vibration frequency, Ω_m, which is the ratio of the angular vibration frequency, ω, to the angular mechanical resonant frequency of the PEH, ω_0. We introduced the normalized extractable power P/P_{lim} of the standard SECE in Fig. 3, where P_{lim} is the maximum harvestable power as defined in [10]. Fig.4 shows the same analysis for the capacitive tuning approach, which consists in adapting the resistive and

capacitive load of a PEH in order to tune its stiffness, as extensively explained in [9]. Finally, the results of the proposed SC-SECE approach are depicted in Fig.5.
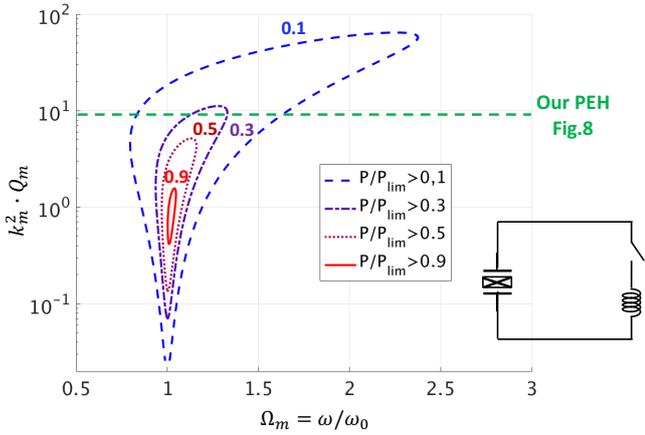

Fig. 3. Normalized analysis of the harvested power with a standard SECE interface [2-4] in the $k_m^2 Q_m$-Ω_m plane, where $Q_m = 20$.
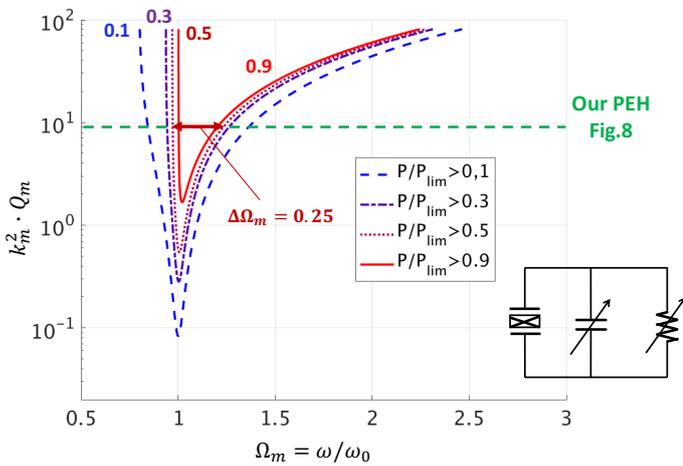

Fig. 4. Normalized analysis of the harvested power with a capacitive tuning interface [9] in the $k_m^2 Q_m$-Ω_m plane where $Q_m = 20$.
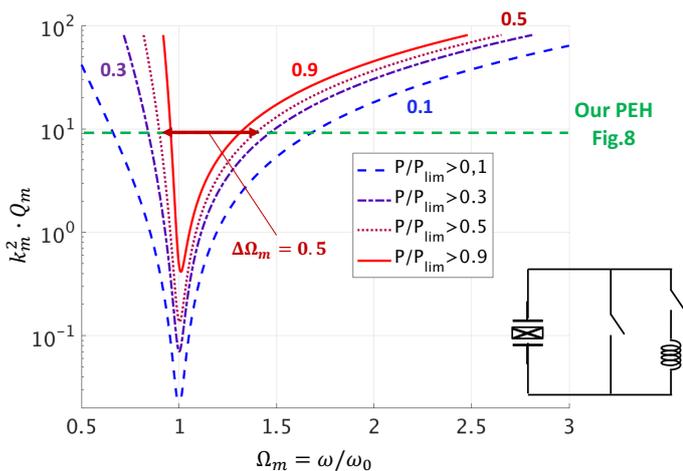

Fig. 5. Normalized analysis of the harvested power thanks to the proposed SC-SECE interface in the $k_m^2 Q_m$-Ω_m plane where $Q_m = 20$.

We can verify from Fig.3 that the SECE interface is only fully efficient when both the product $k_m^2 Q_m$ is about $\pi/4$ and Ω_m is about 1 [2]. Thus, this strategy is sensitive to both external conditions (vibration frequency) and the intrinsic characteristics of the PEH (k_m^2 and Q_m). The capacitive tuning strategy improves the robustness of the system with respect to the vibration frequency. However, this approach requires the use of a bulky capacitive bank. Finally, Fig. 5 shows that the proposed SC-SECE strategy greatly enhances the frequency tuning range compared to other approaches, while continuing to provide a maximal power close to the power limit P$_{lim}$ of any PEH.

In order to evaluate the SC-SECE performance, a new FoM is established (8). This represents the integral of the power frequency response with one strategy compared to that of an optimized resistive load. The maximum harvestable power as well as the FoM are shown on Figures 6 and 7 for the different strategies. For lowly-coupled/highly-damped PEHs, the SECE and SC-SECE are the most effective. When $k_m^2 Q_m$ is higher than $\pi/4$, the maximum harvested power with the SECE strategy starts decreasing while the two other strategies reach P$_{lim}$ for $k_m^2 Q_m \geq \pi$ for the capacitive tuning and for $k_m^2 Q_m \geq \pi/4$ for the SC-SECE strategies. For any $k_m^2 Q_m$, the SC-SECE exhibits a higher FoM than any other strategies.

$$FoM = \frac{\int_0^\infty P_{strategy}(\omega)d\omega}{\int_0^\infty P_{dc}(\omega)d\omega} \qquad (8)$$
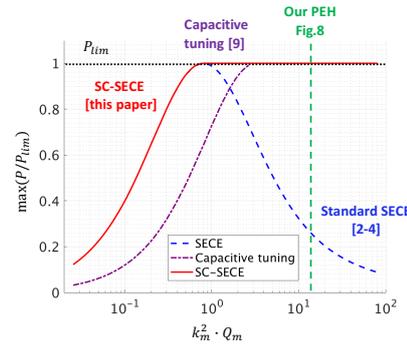

Fig. 6. Maximum harvestable power as a function of $k_m^2 Q_m$ with the standard SECE interface (blue), the capacitive tuning approach (purple), and the proposed SC-SECE (red).
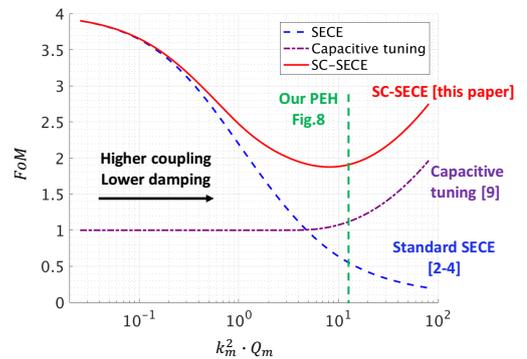

Fig. 7. FoM comparison of the three strategies as a function of $k_m^2 Q_m$
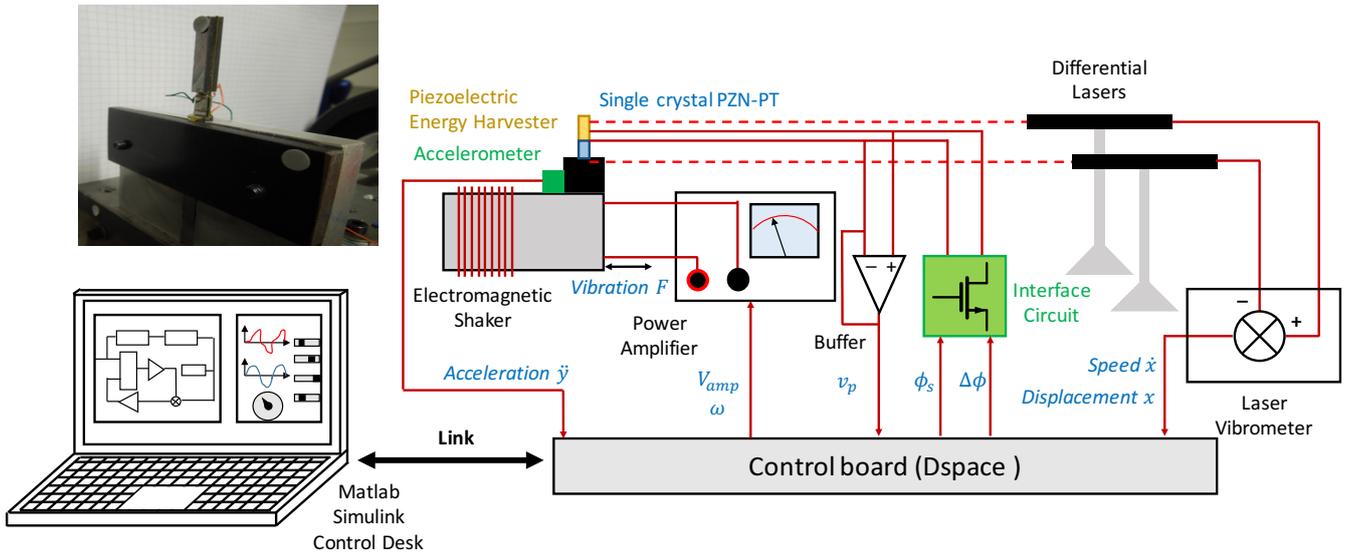
Fig. 8. Experimental setup with automated data collection. The piezoelectric generator is made of 10x5x0.5mm³ plates of PZN-PT single crystals which have been manufactured by Microfine Company.

IV. EXPERIMENTAL VALIDATION

A. Experimental setup

The experimental setup is presented in Fig.8. A highly-coupled piezoelectric generator is fixed on an electromagnetic shaker which vibrates at an angular frequency ω and an amplitude F_m. The mass displacement x and speed $\dot{x}$ are sensed by differential lasers. The piezoelectric voltage waveforms are both memorized and controlled using a Dspace control board dynamically fixing the parameters ϕ_S and $\Delta\phi$. In our experiment, we have collected data for $(\phi_S, \Delta\phi, \omega) \in [0,\pi] \times [0,\pi] \times [565, 943]$, recording precisely $30 \times 30 \times 100$ sets of waveforms.

B. Piezoelectric generator characteristics

The PEH shown in Fig.8 has been characterized: its short-circuit angular frequency $\omega_0 = 628\ \mathrm{rad.s^{-1}}$, squared coupling coefficient $k_m^2 = 0.48$, and quality factor $Q_m = 20$. The piezoelectric capacitance C_p is 1.5 nF. The tests have been performed for a vibration amplitude of 0.03G, and the harvested power limit P_{lim} of our PEH under this vibration is 6μW.

C. Measurement results

The measurement results are presented in Fig.9. The collected data allowed us to plot the maximal harvested power as a function of the vibration frequency, as well as the optimal couples $(\phi_S, \Delta\phi)$ for any vibration frequency. These results can be compared to the theoretical ones which have been obtained by solving (7) with the PEH parameters. As shown in Fig. 9, the experimental results are in good agreement with the model. We observed both theoretically and experimentally, that for some frequencies, two optimal couples $(\phi_S, \Delta\phi)$ which maximize the harvested power can be found. Combined with our highly-coupled PEH, the SC-SECE strategy allowed us to harvest more than 50% of the maximum harvestable power P_{lim} on a relative frequency range $\Delta\omega/\omega_0$ as large as 50%, from 90Hz to 140Hz, which is more than any other reported energy harvesting strategy.
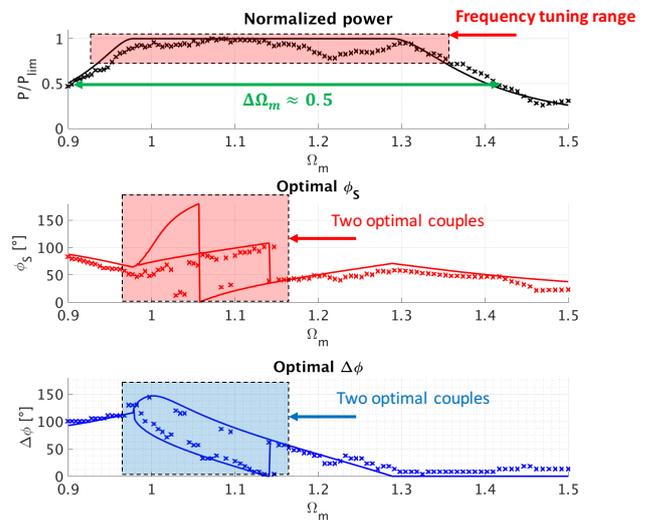

Fig. 9. Experimental (dots) and theoretical (plain lines) maximum harvested power results and optimal $(\phi_S, \Delta\phi)$.

CONCLUSION

In this paper, we propose a new extraction strategy called SC-SECE. By adjusting both the energy harvesting event phase, and the length of a short circuit, this strategy allows the harvested energy to be optimized while tuning the system's electromechanical resonant frequency over a large frequency range. For our PEH (Fig.8), the proposed SC-SECE increases the harvestable energy bandwidth by about 200% compared to a previously proposed capacitive-based tunable interface [9]. In order to implement this strategy in an adaptive interface, the main remaining challenge is to design an algorithm which dynamically determines the couples $(\phi_S, \Delta\phi)$ which maximize the harvested power. This algorithm, if it successfully combines fast convergence and low power consumption, would lead to an efficient way to tune the resonant frequency of linear piezoelectric harvesters.

REFERENCES

[1] J. Krikke, "Sunrise for energy harvesting products" *IEEE Pervasive Comput.,* vol. 4, issue 1, 2005.

[2] E. Lefeuvre *et al.*, "A comparison between several vibration-powered piezoelectric generators for standalone systems", *Sensors and Actuators A: Physical*, vol. 126, no. 2, pp. 405–416, Feb. 2006.

[3] A. Quelen *et al*., "A 30nA Quiescent 80nW to 14mW Power Range Shock-Optimized SECE-based Piezoelectric Harvesting Interface with 420% Harvested Energy Improvement", *IEEE International Solid State Circuit Conference,* to be published.

[4] T. Hehn *et al.*, "A Fully Autonomous Integrated Interface Circuit for Piezoelectric Harvesters", *IEEE Journal of Solid-State Circuits*, vol. 47, no. 9, pp. 2185–2198, Sep. 2012.

[5] G. A. Rincon-Mora and S. Yang, "Tiny piezoelectric harvesters: Principles, constraints and power conversion", *IEEE Trans. Circuits Syst. I, Reg. Papers*, vol. 63, no. 5, pp. 639-649, May 2016.

[6] A. Morel *et al*., "Regenerative synchronous electrical charge extraction for highly coupled piezoelectric generators", *IEEE Midwest symposium of circuits and systems (MWSCAS) 2017,* 2017.

[7] A. Richter *et al.*, "Tunable interface for piezoelectric energy harvesting", in *2014 IEEE 11th International Multi-Conference on Systems, Signals Devices (SSD14)*, pp. 1–5, 2014.

[8] A. Morel *et al.*, "Active AC/DC control for wideband piezoelectric energy harvesting," *Journal of Physics: Conference Series.* 773, 012059, 2016.

[9] B. Ahmed-Seddik *et al*., "Self-powered resonant frequency tuning for piezoelectric vibration energy harvesters", *Journal of Physics: Conference Series* 476, 012069, 2013.

[10] A. Badel *et al*. "Nonlinear Conditioning Circuits for Piezoelectric Energy Harvesters", in: E. Blokhina, A.E. Aroudi, E. Alarcon, D. Galayko (Eds.), Nonlinearity Energy Harvest. Syst., Springer International Publishing, pp. 321–359, 2016.